THE JOURNAL OF PHYSICAL CHEMISTRY Letters

pubs.acs.org/JPCL Letter

Phase-Sensitive Second-Harmonic Generation of Electrochemical Interfaces

Pengtao Xu, Alice Huang, and Jin Suntivich*

Cite This: J. Phys. Chem. Lett. 2020, 11, 8216–8221 Read Online

ACCESS | Metrics & More | Article Recommendations | Supporting Information

ABSTRACT: The interaction between molecular species and charged interfaces plays an indispensable role in a multitude of electrochemical devices. Yet, very little is understood about the nature of this interaction, in particular, the interfacial electric field. Second-order nonlinear spectroscopy such as second-harmonic generation (SHG) can provide chemical information on these interfacial interactions; however, the phase information has received limited attention in electrochemical SHG studies. Here, we demonstrate that the phase of the SHG is essential to the measurement of the electric field at the electrode−electrolyte interface. Our *in situ* SHG experiment provides strong evidence in support of the parabolic model with complex nonlinear susceptibilities. We conclude that if the absolute phase of the total SHG signal with both $\chi^{(2)}$ and $\chi^{(3)}$ contributions can be obtained, it would be possible to measure the potential of zero charge of any electrochemical material.

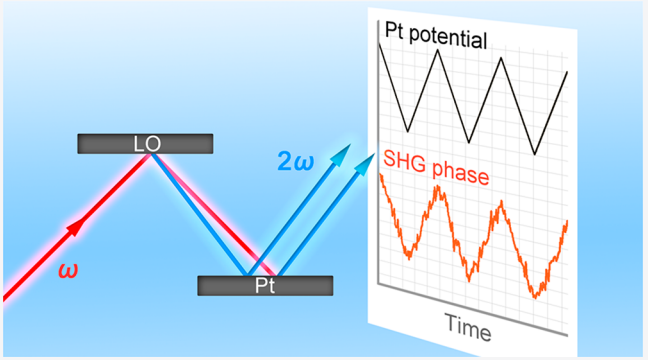

The development of active, efficient electrochemical devices relies on our molecular understanding of electrochemical interfaces, in particular, how the interfacial electric field interacts with molecules on catalytic materials. The Gouy−Chapman−Stern (GCS) model provides a good starting point; however, it is not straightforward to quantify the interfacial electric field in an electrochemical environment. Several reviews[1−3] have highlighted this knowledge gap, including whether the interfacial dipole can influence the electrochemical activities of catalytic metals. It is, therefore, of interest to develop a spectroscopic method that can probe the interfacial electric field in electrochemical experiments. Second-order nonlinear spectroscopy such as SHG offers a powerful way to address these questions owing to their nonlinear origin and well documented methodology.[4−7] However, most electrochemical SHG investigations have thus far focused on the signal intensities rather than phases. Recent SHG investigations on the dielectric−electrolyte interface have shown that phase information is essential to understanding the electrical double layer (EDL). Herein, we examine the role of the SHG phase in electrochemistry, in particular, of the Pt−$HClO_4$ interface that mimics the hydrogen fuel cell and water splitting environments. We discuss how this method can provide an avenue to quantify the potential of zero charge on an electrocatalytic surface, one of the long-standing questions in the electrochemistry field.

SHG describes a conversion of two photons of identical frequency (ω) to one photon of doubled frequency (2ω). Under the electric dipole approximation, this frequency doubling occurs only in a region that is noncentrosymmetric, for example, at the interface of a centrosymmetric crystal and an electrolyte solution. In electroactive environments, the presence of the interfacial electric field can impact SHG, causing the SHG response to depend on the applied potential.[8] Known as the electric field-induced second harmonic (EFISH) effect, the applied field ($\mathbf{E}_{dc}$) can contribute to SHG via the third-order nonlinear optical susceptibility, $\chi^{(3)}$, in the second-order nonlinear polarization, $\mathbf{P}^{(2)}$:

$$\mathbf{P}^{(2)}(2\omega) = (\chi^{(2)} + \chi^{(3)}:\mathbf{E}_{dc}):\mathbf{E}(\omega):\mathbf{E}(\omega) \quad (1)$$

Here $\chi^{(2)}$ is the second-order nonlinear optical susceptibility and $\mathbf{E}(\omega)$ is the electric field of the incoming photon at frequency ω. In this definition, $\mathbf{P}^{(2)}$ of the electrochemical interface represents the sum of all $\chi^{(2)}$ and $\chi^{(3)}$ terms from the solid-electrode surface, surface-bonded species, and EDL.

A number of electrochemical SHG experiments have examined how the SHG signal depends on the applied potential.[9−13] A common observation is the quadratic dependence of the SHG intensity with the electrochemical potential. This empirical behavior is described as the parabolic

Received: August 2, 2020
Accepted: September 3, 2020
Published: September 3, 2020

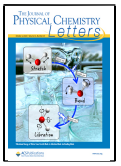

https://dx.doi.org/10.1021/acs.jpclett.0c02364
J. Phys. Chem. Lett. 2020, 11, 8216–8221

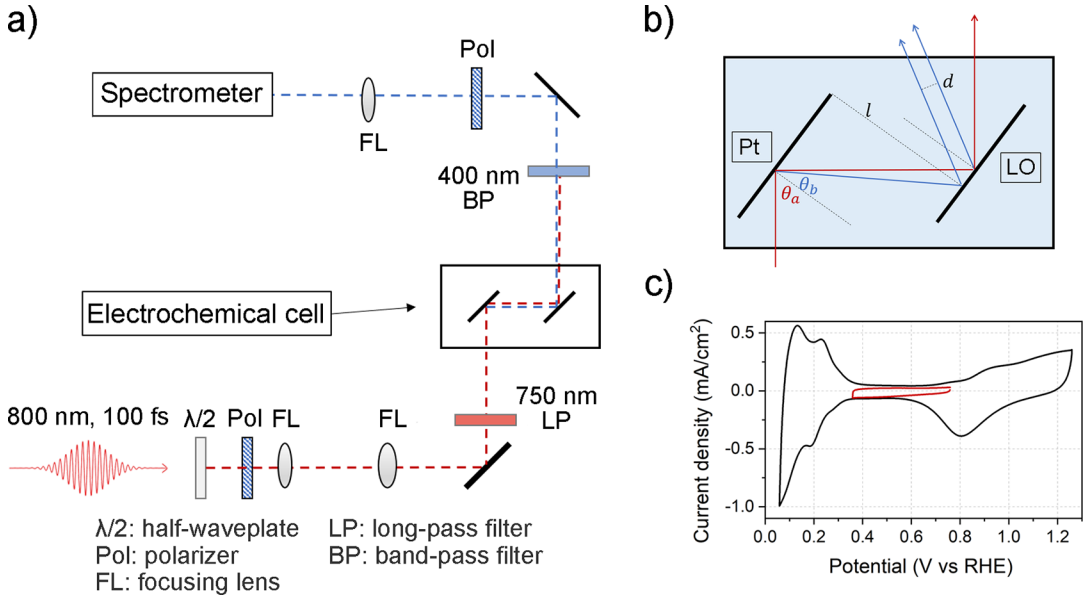

Figure 1. Schematic drawings of (a) our PS-SHG setup and (b) the *in situ* electrochemical SHG cell using a parallel-plate geometry for compensating the SHG beam divergence after the working electrode (Pt) and the local oscillator (LO), where $\theta_a = 45°$. (c) Representative CV of the Pt electrode at 50 mV/s in an Ar-saturated 0.1 M $HClO_4$ aqueous solution. The black and red curves were collected at different potential windows.

model, where the potential at the SHG minimum is often assigned as the potential of zero charge (U_{pzc}). Given that U_{pzc} corresponds to the situation where $\mathbf{E}_{dc} = 0$, this assignment assumes either $\chi^{(3)} \gg \chi^{(2)}$ or their phase angles to differ by 90° (vide infra).[10] However, since it is unclear how valid this assumption is, an alternative way is to measure both the SHG intensity and phase using phase-sensitive SHG (PS-SHG) to obtain U_{pzc}. In PS-SHG measurements, one uses a second SHG signal (local oscillator, LO) to interfere with the sample SHG to retrieve its phase.[14] When the dispersions of the fundamental and the SHG beams are close such as in air, the SHG signals from the sample and LO travel colinearly, leading to a relatively simple interference measurement.[14−17] However, for dispersive media, *e.g.*, water and glass, different refractive indexes of the fundamental and SHG beams prevent the interference from happening. One solution[18,19] is to use a fused silica hemisphere to minimize dispersion. While this method can enable PS-SHG of the fused silica−water interface, the requirement of a transparent substrate is limiting in electrochemical experiments. An alternative approach[20,21] is to make the electrode surface parallel to the glass window of the electrochemical cell. Phase information is then resolved by translating the LO at two positions. However, this method has several drawbacks. First, phase determination using two translation LO positions requires high positioning precision and high laser stability during the translation, which would otherwise generate large errors. Second, the time delay introduced when the pulse propagates through the glass window and the solution requires a compensating element that is not straightforward to incorporate for femtosecond pulses.[18] Third, since the fundamental beams go through the glass−-water interface at a nonzero incident angle, this interface will inevitably contribute to the SHG signal, complicating the analysis.

Here, we report an electrochemical PS-SHG methodology using a simple parallel-plate design that overcomes the optical dispersion issue. Using this setup, we achieve *in situ* PS-SHG at the Pt−$HClO_4$ interface in real time during cyclic voltammetry (CV) measurements. We analyze the origin of the SHG signal by considering the nonlinear contributions from both the EDL and Pt. Simulated SHG signals based on the GCS model suggest that EDL is not the major contributor of the SHG signal. Furthermore, the parabolic model taking into account complex $\chi^{(2)}$ and $\chi^{(3)}$ can well explain the measured data, suggesting that the SHG signal likely arises from the charged layer within the Pt electrode. The parallel-plate design proposed herein can open a new avenue for PS-SHG characterization of any solid−liquid interface to deepen our fundamental understanding of electrochemical interfaces.

The setup for our PS-SHG measurement is shown in Figure 1a. We first confirmed that the SHG signal from the Pt−$HClO_4$ interface (with LO removed) was centered around the second harmonic wavelength of the fundamental beam and exhibited the expected quadratic dependence of its intensity on the input pulse energy (Figure S1).

In dispersive media such as water, the fundamental at an incident angle of θ_b generates SHG at a different angle of θ_b. Using Snell's law, we estimate a 0.4° divergence given the refractive indices of water at the fundamental and SHG frequencies. In the absence of a compensating scheme, this dispersion prevents the SHG signals from the working electrode and LO from interfering. To overcome this issue, we adopted the use of a second Pt electrode parallel to the working electrode as LO in the electrochemical cell (Figure 1b). Both Pt electrodes showed the well-known Pt CV behaviors in different potential regions (Figure 1c, black line): the Pt oxidation ($Pt + H_2O \rightarrow Pt{-}OH + H^+ + e^-$ at >0.6 V vs reversible hydrogen electrode, RHE), EDL (0.4−0.6 V vs RHE), and hydrogen underpotential deposition ($Pt + H^+ + e^- \rightarrow Pt{-}H$ at <0.4 V vs RHE).[22] We focus on the 0.359−0.759 V potential window, where the voltammogram is featureless (Figure 1c, red line) to avoid the contribution from H_{ad} or OH_{ad} electroadsorption, given that our aim is to verify the parabolic model within the GCS limit. In this

https://dx.doi.org/10.1021/acs.jpclett.0c02364
J. Phys. Chem. Lett. 2020, 11, 8216−8221

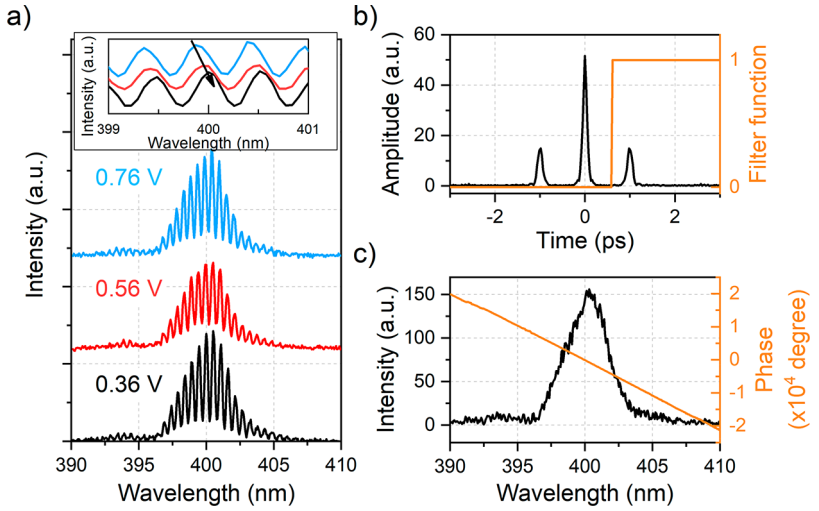

Figure 2. (a) Spectral interferograms of the SHG signals recorded at difference potentials. Inset: enlarged graph highlighting the shifting of the interference fringes with applied potentials. (b) Black line, inverse Fourier-transformed spectrum of the black interferogram in (a); orange line, filter function used to isolate the pulse on the right. (c) Recovered spectral intensity (black) and phase (orange) from a Fourier transform of the filtered pulse.

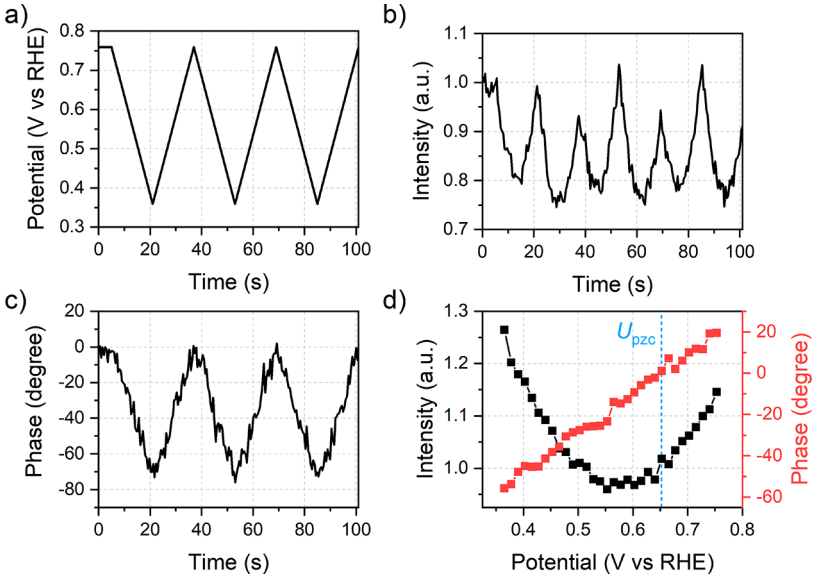

Figure 3. Potential profile (a) for cyclic voltammetry along with the measured SHG intensity (b) and phase (c) change over time. Data is normalized to time = 0. (d) SHG intensity (black) and phase (red) change with potential (averaged over four CV cycles); blue dashed line represents U_{pzc}, which is used as the reference point.

parallel-plate geometry, the reference SHG signal generated from LO co-propagates with the sample SHG with an offset (d, see Figure 1b). Given that the two Pt electrodes are ∼1 cm apart (l), we can estimate $d \approx 0.11$ mm, which is small compared to the beam diameter (∼1.5 mm). Our SHG setup can, therefore, allow LO-sample interference (Figure 2a). It is important to note that the proposed parallel-plate method can be adapted to any nonlinear medium; we use the same material as the working electrode for LO in this work to maximize the interference contrast given their comparable SHG signals.

To extract phase information, several PS-SHG studies[18−21] have used methods based on time-domain interference, where the SHG intensity as a function of the time delay between the SHG generation of the sample and the subsequent interference with the LO is measured. In electrochemical experiments, the time delay (>1 ps) caused by the presence of the dispersive media (*e.g.*, water) between the working electrode and LO makes the temporal overlap of the femtosecond SHG pulses impractical. While this issue could be addressed with a compensator (such as calcite[18]), we use instead a frequency-domain method to retrieve the phases. Compared with the time-domain method, the frequency-domain approach has the advantage of improved time resolution to allow the possibility of a real-time PS-SHG measurement.

Our phase extraction uses a Fourier-transformed algorithm.[23,24] We start with the definition of the SHG intensity (I), which can be described by the following equation (see the Supporting Information for derivation):

$$I = |\mathbf{E}_{Pt}|^2 + |\mathbf{E}_{LO}|^2 + \mathbf{E}_{Pt}\mathbf{E}_{LO}^{*} \exp(i\omega T) + \mathbf{E}_{Pt}^{*}\mathbf{E}_{LO}\exp(-i\omega T) \quad (2)$$

https://dx.doi.org/10.1021/acs.jpclett.0c02364
J. Phys. Chem. Lett. 2020, 11, 8216−8221

where $\mathbf{E}_{Pt}$ and $\mathbf{E}_{LO}$ are the electric fields of the SHG in the frequency domain from the Pt electrode and LO, respectively, and T is the time delay between the two signals. Figure 2b shows the inverse Fourier-transformed intensity, where the feature at $t = 0$ corresponds to the first two terms of eq 2 and the feature at $t = \pm 1$ ps corresponds the last two terms (cross terms). As the two cross terms are responsible for the interference in Figure 2a and the one at $t = 1$ ps contains the correct sign of the sample phase, we extract the information using a Heaviside filter (Figure 2b, orange line). We then apply Fourier transformation to the filtered time-domain spectra to recover the desired cross term, i.e., $\mathbf{E}_{Pt}\mathbf{E}^*_{LO}\exp(i\omega T)$.

To obtain the value of $\mathbf{E}_{Pt}$, one can use a reference material with known nonlinear optical susceptibilities (such as quartz) after the Fresnel factor correction.[17,23] This is the subject of our future research. For this work, we focus our effort on the relative change of the SHG as a function of the electrochemical potential to first validate the parabolic model. In this approach, we normalize the SHG to the value at a fixed potential (U_0):

$$I_{eff} = \frac{I(U)}{I(U_0)} \propto \frac{|\mathbf{E}_{Pt}(U)\mathbf{E}^*_{LO}\exp(i\omega T)|}{|\mathbf{E}_{Pt}(U_0)\mathbf{E}^*_{LO}\exp(i\omega T)|} = \frac{|\mathbf{E}_{Pt}(U)|}{|\mathbf{E}_{Pt}(U_0)|} \quad (3)$$

We use this normalization scheme in our report of the SHG intensity and phase as a function of the potential U. We chose the U_{pzc} of the Pt surface as the reference U_0 point in the same electrolyte (0.65 V vs RHE) determined from electrochemical impedance spectroscopy (see the Supporting Information).

We observed the real-time change in the SHG response when scanning the electrochemical potential in the EDL region (Figure 3). In each CV cycle, the SHG intensity shows two peaks on the time axis while the SHG phase directly tracks the applied potential. When plotted on the potential axis, the SHG intensity and phase show a parabolic and a linear relationship with the applied electrochemical potential, respectively. It is important to note that the ability to do real-time SHG measurements allows us to correct for the drift of the phase (Figure S4), which is likely a result of the mechanical instability of the LO. We have corrected this drift in our SHG-phase analysis (Figure 3) using an interpolated linear background.

The solid-electrode surface, the surface-bonded species, and the EDL can contribute to the SHG; we analyze how each of these factors could serve as the origin of the observed potential-dependent PS-SHG. Starting from the liquid side (EDL), if the measured nonlinear response solely originates from the aqueous region, the GCS theory[25] can be used to calculate its contribution to the SHG (see calculation details in the Supporting Information). Under the off-resonant assumption, where the complex nonlinear susceptibilities are real, we found that irrespective of whichever $\chi^{(2)}$ and $\chi^{(3)}$ values were assumed, the simulated potential-dependent SHG response from eq S10 could not replicate the PS-SHG results (Figure 4 shows an example of $\chi^{(3)}/\chi^{(2)} = 5\ V^{-1}$). This is because the phase contribution from the EDL came from the phase mismatch (eq S10), which, for concentrated solutions such as 0.1 M $HClO_4$, is too small. In solutions with high ionic strengths, $\mathbf{E}_{dc}$ decays rapidly at the solid−liquid interface (Figure S5). As a result, the interference depth of the optical field is only a few layers of water molecules[26] and the small phase change from the calculation cannot explain the SHG phase shift in Figure 3. Having ruled out the GCS contribution to the observed SHG, we next eliminate the contribution from the surface-bonded species, given that the examined potential window is above the hydrogen underpotential deposition and below the water oxidation on Pt, *i.e.*, corresponds to the potential with no surface bound species.

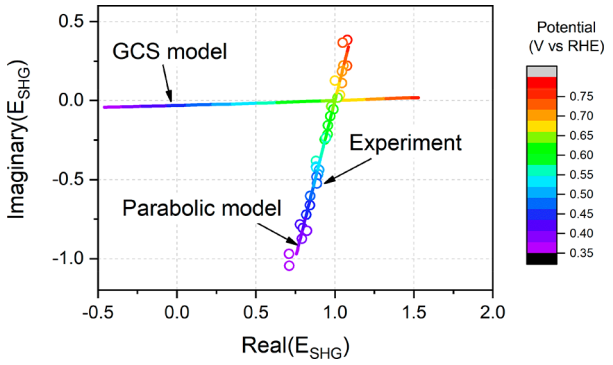

Figure 4. Complex plane representation of the SHG electric field ($\mathbf{E}_{SHG}$) measured experimentally (circles) and simulated numerically (lines) using the GCS model and the parabolic model. All the data are normalized to the value at U_{pzc}.

We next consider the nonlinear response from the solid Pt electrode. Unlike dielectrics, metallic surfaces usually exhibit complex nonlinear susceptibilities. To factor in the possibility of complex $\chi^{(2)}$ and $\chi^{(3)}$, we define $\alpha e^{i\theta} = \chi^{(2)}/\chi^{(3)}$, where and θ represent the magnitude ratio and relative phase between $\chi^{(2)}$ and $\chi^{(3)}$, respectively. Substituting this definition into eq 1, we can express the electric field of the SHG as

$$\mathbf{E}_{Pt}(U) \propto \alpha\, e^{i\theta} + U - U_{pzc} \quad (4)$$

This equation, which is known as the parabolic model, has been used to explain how the applied potential impacts the SHG in the EFISH effect. Fitting the experimental SHG data with eq 4 using the least-squares minimization, we obtained an outstanding fit both in the real and imaginary axes of the SHG response ($\alpha = -0.286 \pm 0.003$, $\theta = 104.3 \pm 0.6°$, $R^2 = 0.998$), as shown in Figure 4. The excellent agreement with our experimental data suggests the solid Pt electrode dominates the SHG response, not the EDL that is commonly assumed in the dielectric−electrolyte interface. We rationalize this observation by pointing out that $\chi^{(3)}$ of metallic materials (*e.g.*, 10^{-19} m^2/V^2 for Au)[27] is much larger than that of water (10^{-22} m^2/V^2).[28] Most critically, our work shows that if either α or θ is known, one can use eq 4 to directly determine U_{pzc}. This determination can be achieved by measuring the absolute phase with a standard nonlinear reference like alpha-quartz or using clever optical methods like multiple-angle heterodyne detection.[29] Given the importance of U_{pzc} in our understanding of the electrode−electrolyte structure and the interfacial electron transfer process,[30−32] we envision this experiment as the next important step of the electrochemical SHG studies. Finally, we note that, as with the previous studies,[9−13] the SHG intensity minimum is close to U_{pzc} in our experiment (Figure 3d). This observation suggests that $\chi^{(2)}$ and $\chi^{(3)}$ may be orthogonal for Pt. In fact, the fitted θ is close to 90°. When $\theta = 90°$, the SHG intensity minimum occurs at $U = U_{pzc}$ according to the parabolic model (see Figure S7 for details). We emphasize however this observation does not suggest that one should use the minimum of the SHG intensity to determine U_{pzc} since there is no evidence supporting the orthogonality between $\chi^{(2)}$ and $\chi^{(3)}$. As discussed in this work, the right approach is to measure the complex $\chi^{(2)}$ and $\chi^{(3)}$ and find U

https://dx.doi.org/10.1021/acs.jpclett.0c02364
J. Phys. Chem. Lett. 2020, 11, 8216−8221

where $\chi^{(3)}$ vanishes; this approach is applicable to all materials without having to relying on the assumption of orthogonal $\chi^{(2)}$ and $\chi^{(3)}$.

In conclusion, we report an *in situ* PS-SHG configuration using a parallel-plate geometry. This setup overcomes the optical dispersion at the interface and allows for a rapid retrieval of the SHG phase information through the frequency-domain interference. We applied this technique to a Pt−$HClO_4$ interface under electrochemical conditions. We found that the GCS model cannot explain the observed SHG phase even though we have limited our analysis within the potential window in the capacitive area (where the GCS theory is valid). Instead, the SHG signal comes from the nonlinear response of the Pt electrode surface rather than the interfacial solvent, because the observed SHG response is consistent with the parabolic model that has been used to explain the EFISH effect. We attribute this observation to the larger nonlinear susceptibilities of metal compared to water. Our work indicates that, with the absolute phase information on the nonlinear optical susceptibilities, one can measure the potential of zero charge for any electrode material. This work demonstrates a novel strategy for measuring PS-SHG at metal−electrolyte interfaces. We believe that this advance can contribute to a more in-depth investigation of the interfacial electrochemistry in the future.

EXPERIMENTAL SECTION

Optical Setup. The light source in our phase-sensitive SHG experiments was a regenerative amplifier (Spectra-Physics, Spitfire Ace) pumped by a 100 fs Ti:sapphire oscillator (Spectra-Physics, MaiTai). The fundamental input was set at 800 nm with a full width at half-maximum of 13 nm and a repetition rate of 1 kHz. Before the sample stage, the fundamental beam was focused to a beam diameter of ∼1.5 mm through a set of focal lenses (F = 20 cm and F = 5 cm), followed by a 750 nm long-pass filter (Thorlabs) to remove any second harmonic co-propagating within. The pulse energy arriving at the electrochemical cell was 130 μJ. The pulse after the cell was filtered with a 400 nm bandpass filter and directed though a second polarizer and then detected by a spectrometer (Princeton Instruments, SP-2500) equipped with a 600 lines/mm grating (blaze 500 nm) and a thermoelectric-cooled charge-coupled device (CCD, Princeton Instruments, PIXIS 400). A polarization combination of p-in and p-out was used. The exposure time used for each frame was 0.5 s.

Electrochemical Measurements. A glass cuvette (93G20, FireflySci, Inc.) was customized as a three-electrode cell with Ag/AgCl (4.0 M NaCl) as the reference electrode and a Pt wire as the counter electrode. All the potentials reported in the paper were referred to the RHE scale by E(V vs RHE) = 0.259 + E(V vs Ag/AgCl), which was calibrated using Pt/H_2. The working electrode was made by cutting a Pt-coated glass slide (100 nm Pt with 5 nm Ti as binding layer, Platypus Technologies) into a 1 cm × 2.5 cm piece, which was then attached to a titanium wire using silver paint (Ted Pella, Leitsilber 200) and insulated with epoxy (Omegabond 101). The active area of the working electrode was 0.36 cm^2. The electrolyte was 0.1 M $HClO_4$, which was purged with Ar throughout the experiment. Pt electrodes were electrochemically cleaned using a Bio-Logic SP-300 potentiostat by cyclic voltammetry until the curve was stabilized. *In operando* SHG measurements were done using an EC301 potentiostat (Stanford Research Systems) integrated with Python interface for synchronization. Details on the measurement and analysis of electrochemical impedance spectroscopy (EIS) are provided in the Supporting Information.

ASSOCIATED CONTENT

Supporting Information

The Supporting Information is available free of charge at https://pubs.acs.org/doi/10.1021/acs.jpclett.0c02364.

SHG spectrum of the Pt−$HClO_4$ interface and its intensity change with pulse energy, derivation of eq 2, EIS measurement of U_{pzc}, SHG intensity and phase stability over time, wavevector mismatch calculation, calculation of SHG response from the electrochemical double layer, and graphic representation of eq 4 (PDF)

AUTHOR INFORMATION

Corresponding Author

Jin Suntivich − *Department of Materials Science and Engineering and Kavli Institute at Cornell for Nanoscale Science, Cornell University, Ithaca, New York 14853, United States;* orcid.org/0000-0002-3427-4363; Email: jsuntivich@cornell.edu

Authors

Pengtao Xu − *Department of Materials Science and Engineering, Cornell University, Ithaca, New York 14853, United States;* orcid.org/0000-0002-4470-446X

Alice Huang − *School of Engineering and Applied Physics, Cornell University, Ithaca, New York 14853, United States*

Complete contact information is available at: https://pubs.acs.org/10.1021/acs.jpclett.0c02364

Notes

The authors declare no competing financial interest.

ACKNOWLEDGMENTS

This work was supported as part of the Center for Alkaline-Based Energy Solutions (CABES), an Energy Frontier Research Center funded by the U.S. Department of Energy, Office of Science, Office of Basic Energy Sciences, under Award No. DE-SC0019445. J.S. acknowledges support of the Sloan Research Fellowship from the Alfred P. Sloan Foundation. We thank Jie Shan and Aaron Lindenberg for helpful discussion on the experimental setup and EFISH phenomena.

REFERENCES

(1) Björneholm, O.; Hansen, M. H.; Hodgson, A.; Liu, L.-M.; Limmer, D. T.; Michaelides, A.; Pedevilla, P.; Rossmeisl, J.; Shen, H.; Tocci, G.; et al. Water at Interfaces. *Chem. Rev.* **2016**, *116*, 7698−7726.

(2) Chen, L. D.; Urushihara, M.; Chan, K.; Nørskov, J. K. Electric Field Effects in Electrochemical CO_2 Reduction. *ACS Catal.* **2016**, *6*, 7133−7139.

(3) Tian, X.; Zhao, P.; Sheng, W. Hydrogen Evolution and Oxidation: Mechanistic Studies and Material Advances. *Adv. Mater.* **2019**, *31*, 1808066.

(4) Shen, Y. R. Surface Properties Probed by Second-Harmonic and Sum-Frequency Generation. *Nature* **1989**, *337*, 519−525.

(5) Eisenthal, K. B. Liquid Interfaces Probed by Second-Harmonic and Sum-Frequency Spectroscopy. *Chem. Rev.* **1996**, *96*, 1343−1360.

(6) Ge, A.; Rudshteyn, B.; Videla, P. E.; Miller, C. J.; Kubiak, C. P.; Batista, V. S.; Lian, T. Heterogenized Molecular Catalysts: Vibrational

Sum-Frequency Spectroscopic, Electrochemical, and Theoretical Investigations. *Acc. Chem. Res.* **2019**, *52*, 1289−1300.
(7) Tang, F.; Ohto, T.; Sun, S.; Rouxel, J. R.; Imoto, S.; Backus, E. H. G.; Mukamel, S.; Bonn, M.; Nagata, Y. Molecular Structure and Modeling of Water−Air and Ice−Air Interfaces Monitored by Sum-Frequency Generation. *Chem. Rev.* **2020**, *120*, 3633−3667.
(8) Lee, C. H.; Chang, R. K.; Bloembergen, N. Nonlinear Electroreflectance in Silicon and Silver. *Phys. Rev. Lett.* **1967**, *18*, 167−170.
(9) Corn, R. M.; Romagnoli, M.; Levenson, M. D.; Philpott, M. R. The Potential Dependence of Surface Plasmon-Enhanced Second-Harmonic Generation at Thin Film Silver Electrodes. *Chem. Phys. Lett.* **1984**, *106*, 30−35.
(10) Guyot-Sionnest, P.; Tadjeddine, A. Study of Ag(111) and Au(111) Electrodes by Optical Second-harmonic Generation. *J. Chem. Phys.* **1990**, *92*, 734−738.
(11) Aktsipetrov, O. A.; Melnikov, A. V.; Murzina, T. V.; Nikulin, A. A.; Rubtsov, A. N. DC-Electric-Field-Induced Optical Second Harmonic Generation at the Smooth Metal-Electrolyte Interface. *Surf. Sci.* **1995**, *336*, 225−231.
(12) Bian, H.-T.; Guo, Y.; Wang, H.-F. Non-Parabolic Potential Dependence of Optical Second Harmonic Generation from the Si(111) Electrode/Electrolyte Interface. *Phys. Chem. Chem. Phys.* **2018**, *20*, 29539−29548.
(13) Daschbach, J. L.; Fischer, P. R.; Gragson, D. E.; Richmond, G. L. Observation of the Potential-Dependent Second Harmonic Response from the Si(111)/Electrolyte and Si(111)/SiO_2/Electrolyte Interfacial Regions. *J. Phys. Chem.* **1995**, *99*, 3240−3250.
(14) Stolle, R.; Marowsky, G.; Schwarzberg, E.; Berkovic, G. Phase Measurements in Nonlinear Optics. *Appl. Phys. B: Lasers Opt.* **1996**, *63*, 491−498.
(15) Chang, R. K.; Ducuing, J.; Bloembergen, N. Relative Phase Measurement between Fundamental and Second-Harmonic Light. *Phys. Rev. Lett.* **1965**, *15*, 6−8.
(16) Lepetit, L.; Chériaux, G.; Joffre, M. Linear Techniques of Phase Measurement by Femtosecond Spectral Interferometry for Applications in Spectroscopy. *J. Opt. Soc. Am. B* **1995**, *12*, 2467.
(17) Shen, Y. R. Phase-Sensitive Sum-Frequency Spectroscopy. *Annu. Rev. Phys. Chem.* **2013**, *64*, 129−150.
(18) Ohno, P. E.; Chang, H.; Spencer, A. P.; Liu, Y.; Boamah, M. D.; Wang, H.; Geiger, F. M. Beyond the Gouy−Chapman Model with Heterodyne-Detected Second Harmonic Generation. *J. Phys. Chem. Lett.* **2019**, *10*, 2328−2334.
(19) Chang, H.; Ohno, P. E.; Liu, Y.; Lozier, E. H.; Dalchand, N.; Geiger, F. M. Direct Measurement of Charge Reversal on Lipid Bilayers Using Heterodyne-Detected Second Harmonic Generation Spectroscopy. *J. Phys. Chem. B* **2020**, *124*, 641−649.
(20) Pettinger, B.; Bilger, C. A Novel Approach to Analyze the Optical Second Harmonic Generation Anisotropy at Surfaces Employing Interference Techniques. Example: The Au(110) Electrode. *Chem. Phys. Lett.* **1998**, *286*, 355−360.
(21) Pettinger, B.; Bilger, C.; Beltramo, G.; Santos, E.; Schmickler, W. Interference Second Harmonic Anisotropy at Single Crystalline Silver-Electrodes. *Electrochim. Acta* **1998**, *44*, 897−901.
(22) Sheng, W.; Gasteiger, H. A.; Shao-Horn, Y. Hydrogen Oxidation and Evolution Reaction Kinetics on Platinum: Acid vs Alkaline Electrolytes. *J. Electrochem. Soc.* **2010**, *157*, B1529.
(23) Yamaguchi, S.; Tahara, T. Heterodyne-Detected Electronic Sum Frequency Generation: "Up" versus "Down" Alignment of Interfacial Molecules. *J. Chem. Phys.* **2008**, *129*, 101102.
(24) Nihonyanagi, S.; Yamaguchi, S.; Tahara, T. Direct Evidence for Orientational Flip-Flop of Water Molecules at Charged Interfaces: A Heterodyne-Detected Vibrational Sum Frequency Generation Study. *J. Chem. Phys.* **2009**, *130*, 204704.
(25) Bard, A. J.; Faulkner, L. R. *Electrochemical Methods: Fundamentals and Applications*, 2nd ed.; Wiley and Sons, 2000.
(26) Gonella, G.; Lütgebaucks, C.; de Beer, A. G. F.; Roke, S. Second Harmonic and Sum-Frequency Generation from Aqueous Interfaces Is Modulated by Interference. *J. Phys. Chem. C* **2016**, *120*, 9165−9173.
(27) Boyd, R. W.; Shi, Z.; De Leon, I. The Third-Order Nonlinear Optical Susceptibility of Gold. *Opt. Commun.* **2014**, *326*, 74−79.
(28) Dalstein, L.; Chiang, K.-Y.; Wen, Y.-C. Direct Quantification of Water Surface Charge by Phase-Sensitive Second Harmonic Spectroscopy. *J. Phys. Chem. Lett.* **2019**, *10*, 5200−5205.
(29) Yang, W. C.; Busson, B.; Hore, D. K. Determining Nonlinear Optical Coefficients of Metals by Multiple Angle of Incidence Heterodyne-Detected Sum-Frequency Generation Spectroscopy. *J. Chem. Phys.* **2020**, *152*, 084708.
(30) Ledezma-Yanez, I.; Wallace, W. D. Z.; Sebastián-Pascual, P.; Climent, V.; Feliu, J. M.; Koper, M. T. M. Interfacial Water Reorganization as a pH-Dependent Descriptor of the Hydrogen Evolution Rate on Platinum Electrodes. *Nat. Energy* **2017**, *2*, 17031.
(31) Ryu, J.; Surendranath, Y. Tracking Electrical Fields at the Pt/H_2O Interface during Hydrogen Catalysis. *J. Am. Chem. Soc.* **2019**, *141*, 15524−15531.
(32) Ojha, K.; Arulmozhi, N.; Aranzales, D.; Koper, M. T. M. Double Layer at the Pt(111)−Aqueous Electrolyte Interface: Potential of Zero Charge and Anomalous Gouy−Chapman Screening. *Angew. Chem., Int. Ed.* **2020**, *59*, 711−715.

https://dx.doi.org/10.1021/acs.jpclett.0c02364
J. Phys. Chem. Lett. 2020, 11, 8216−8221